

Multi-scale Simulations of Metal-Semiconductor Nanoscale Contacts

This content has been downloaded from IOPscience. Please scroll down to see the full text.

2015 J. Phys.: Conf. Ser. 647 012030

(<http://iopscience.iop.org/1742-6596/647/1/012030>)

View [the table of contents for this issue](#), or go to the [journal homepage](#) for more

Download details:

IP Address: 144.173.57.69

This content was downloaded on 22/06/2016 at 17:14

Please note that [terms and conditions apply](#).

Multi-scale Simulations of Metal-Semiconductor Nanoscale Contacts

M. Aldegunde¹, S. P. Hepplestone², P. V. Sushko³ and K. Kalna⁴

¹Warwick Centre for Predictive Modelling, School of Engineering, University of Warwick, Coventry CV4 7AL, UK.

²Deregallera Ltd., Caerphilly CF83 2HU, Wales, UK.

³ Pacific Northwest National Laboratory, Richland, WA 99352, USA.

⁴Electronic Systems Design Centre, Swansea University, Swansea SA2 8PP, Wales, UK.

E-mail: k.kalna@swansea.ac.uk

Abstract. An electron transport simulations via a metal-semiconductor interface is carried out using multi-scale approach by coupling ab-initio calculations with 3D finite element ensemble Monte Carlo technique. The density functional theory calculations of the Mo/GaAs (001) interface show electronic properties of semiconductor dramatically change close to the interface having a strong impact on the transport. Tunnelling barrier lowers and widens due to a band gap narrowing near the interface reducing resistivity by more than one order of magnitude: from $2.1 \times 10^{-8} \Omega \cdot \text{cm}^2$ to $4.7 \times 10^{-10} \Omega \cdot \text{cm}^2$. The dependence of electron effective mass from the distance to the interface also plays a role bringing resistivity to $7.9 \times 10^{-10} \Omega \cdot \text{cm}^2$.

1. Introduction

Metal-semiconductor contacts are integral components of any semiconductor device. When these devices are scaled to nanometer dimensions, transport through the contacts becomes affected by their atomic structure and atomic-scale variations of their electronic properties. Here, we present a multi-scale approach, in which the results of ab-initio calculations of a metal-semiconductor interface are mapped onto semi-classical transport simulations performed using a three-dimensional (3D) self-consistent finite element ensemble Monte Carlo method with atomic resolution. We demonstrate this approach on a Mo/GaAs(100) interface [1], a candidate for the source/drain contacts in III-V MOSFETs for future sub-16 nm CMOS technologies [2].

2. The Multiscale Computational Method

We use a two-level hierarchical method for predicting electrical current through a metal-semiconductor contact. The first level is based on the density functional theory (DFT) calculations to obtain the geometrical structure and electronic properties. The results allow to define characteristic electronic structure parameters, such as effective electron mass, as functions of the distance from the interface, which then transferred into semiclassical ensemble Monte Carlo transport simulations [3, 4].

2.1. Density Functional Theory Calculations

The Mo/GaAs (100) interface is modelled as a periodic heterostructure of an eight-bilayer thick slab of GaAs and a five monolayer thick slab of Mo, both terminated with (100) planes. The



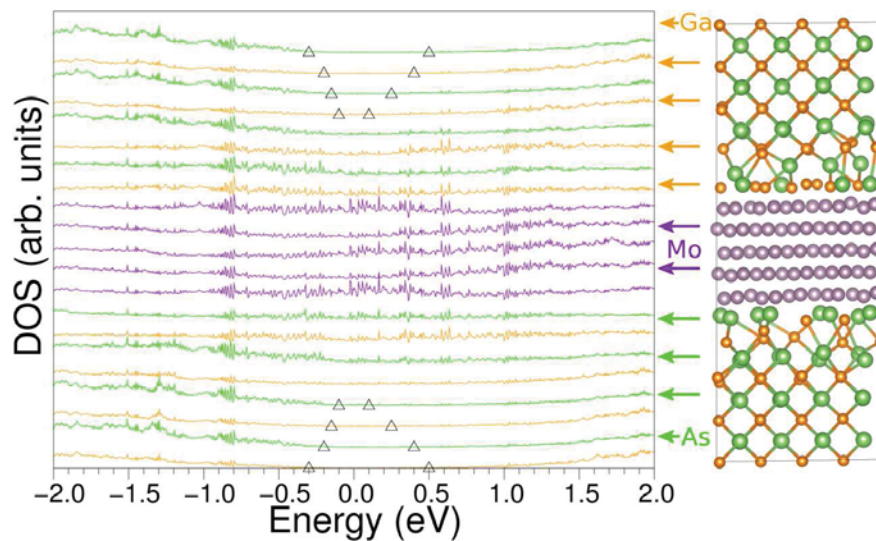


Figure 1. Layer averaged projected density of states (LPDOS)

Mo part of it was rotated by 33.7° around the axis perpendicular to the plane of the interface, resulting in lattice mismatch of less than 3%. We use the density functional by Perdew, Burke and Ernzerhof (PBE) [5] and the projected augmented waves method [6], as implemented in the Vienna ab-initio package (VASP) [7]. The total energy of the system was minimized with respect to coordinates of all atoms and the cell parameters. A combination of the conjugate gradient method and ab initio molecular dynamics, based on the Verlet algorithm, the cutoff of 450 eV and a $3 \times 3 \times 1$ Monkhorst-Pack k -point set were used for these calculations. The atom-projected density of states (PDOS) was calculated for the relaxed super-cell using the cutoff of 500 eV and a $5 \times 5 \times 2$ k -point set. Fig. 1 shows the geometric structure and density of states projected on atoms of each atomic plane in the Mo/GaAs (100) heterostructure. Analysis of the PDOS demonstrates the band gap narrowing and the presence of the metal induced gap states on both Ga- and As-terminated interfaces of GaAs with the Mo film, which we attribute to the charge density redistribution at the interface.

To find the dependence of the electron effective mass (m^*) in GaAs on the distance from the interface, we assume that the local value of m^* is determined by the local band gap, as defined using PDOS in Fig. 1. In turn, the value of the band gap correlates well with the GaAs lattice constant. Therefore, we first calculated the one-electron band gaps and the corresponding effective masses for several values of the lattice constants of the bulk GaAs. The CRYSTAL09 package [8], the Gaussian-type DEF2 basis set [9] and the PBE functional [5] were used in these calculations. The obtained values were recalculated to the distance from the interface and referenced to the bulk band gap and the electron mass. The band gap decreases linearly and disappears two bilayers away from the interface. Similarly, the electron effective mass decreases and becomes undefined when the gap closes.

2.2. Mapping of Material Parameters in Multiscale Approach

The variations of the conduction and valence band edges with respect to the Fermi level (Fig. 1) and the electron effective mass [10] were mapped into a 3D ensemble Monte Carlo transport simulation. It has been enhanced with a tunnelling transport model [11, 12] to treat the transport through the metal-semiconductor interface [13]. The reduction of the band gap (Fig. 2) changes the Schottky barrier, both its height and shape (Fig. 4). This affects dramatically tunnelling

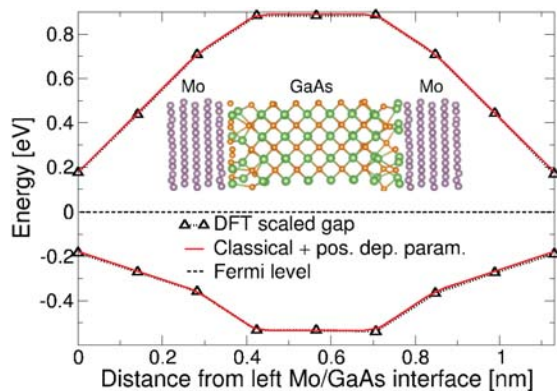


Figure 2. Conduction and valence band edges extracted from the DFT simulation (black diamond dotted line) for the position dependent parameters (continuous red line).

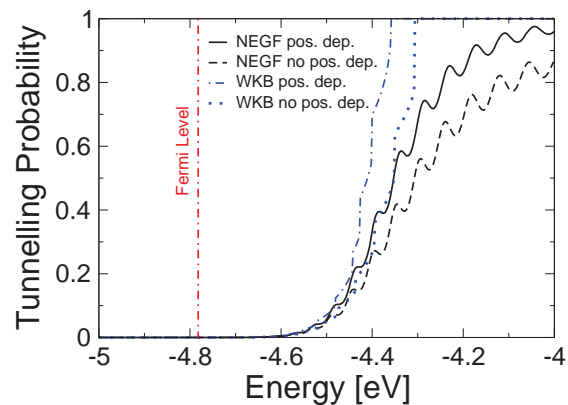


Figure 3. Tunnelling probabilities extracted from a 3D simulation of a Mo/ n^+ -GaAs interface for NEGF and WKB approximations.

probability at the interface as illustrated in Fig. 3. In addition, a small reduction in the mass of the electrons due to the local strain will further affects the probability. These changes in material characteristics of the interface impact the electrostatics through the self-consistent solution of 3D Poisson equation [4] which also takes into account the barrier lowering induced by the static image charge [14] as shown in Fig. 4.

2.3. Monte Carlo Simulated Transport Through Metal-Semiconductor Interface

To test our methodology, we have chosen a Mo/ n^+ -GaAs interface with a very high GaAs n -type doping of $5 \times 10^{19} \text{cm}^{-3}$. The high doping provides a very thin barrier which leads to the Ohmic behaviour of the contact. Such high doping can be fabricated using laser assisted annealing or rapid thermal annealing (RTA) [15]. The doping density of $4.5 \times 10^{19} \text{cm}^{-3}$ has been also reported in 30 nm gate length enhancement mode $\text{In}_{0.53}\text{Ga}_{0.47}\text{As}$ MOSFETs [16].

We simulate the contact resistivity using four different approaches to evaluate the impact of the two sources of the position dependent parameters: (i) no position dependent parameters, (ii) position dependence only for the electron effective mass, (iii) position dependence only for the conduction band and (iv) position dependences in both the electron effective mass and the conduction band. Note that the 3D ensemble Monte Carlo simulations were verified to provide the correct electron mobility in bulk materials. A contact resistivity of $2.1 \times 10^{-8} \Omega \cdot \text{cm}^2$ was obtained using no position dependent parameters. The simulations with position dependent bands and masses has given a contact resistivity of $7.9 \times 10^{-10} \Omega \cdot \text{cm}^2$, of $2.0 \times 10^{-8} \Omega \cdot \text{cm}^2$ using only position dependent electron effective masses and, finally, of $4.7 \times 10^{-10} \Omega \cdot \text{cm}^2$ using only position dependent bands.

3. Conclusions

In this work, we presented a hierarchical simulation model for predicting transport characteristics of metal-semiconductor interfaces. The electronic structure near the interface is calculated using DFT and the obtained variations of the conduction and valence band edges and the electron effective mass are then mapped into a semiclassical transport module within the 3D finite element self-consistent ensemble Monte Carlo technique enhanced with a tunnelling transport model. The resistivity of the Mo/ n^+ -GaAs contact is then investigated. We have found that the impact of the narrowing of the semiconductor band gap in the close vicinity of the interface

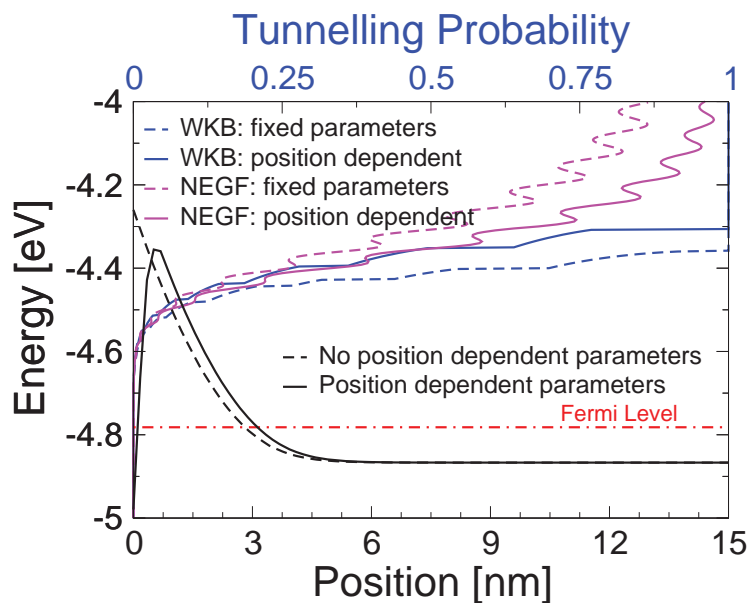


Figure 4. Conduction band and tunnelling probability obtained using position dependent (continuous line) and constant bulk material parameters (dashed line).

is a major reason for the modification of the contact resistivity. The band gap narrowing in semiconductor side of the interface reduces the resistivity by more than one order of magnitude: from $2.1 \times 10^{-8} \Omega \cdot \text{cm}^2$ to $4.7 \times 10^{-10} \Omega \cdot \text{cm}^2$. The position dependence of the electron effective mass is also playing an important role leading to a total resistivity of $7.9 \times 10^{-10} \Omega \cdot \text{cm}^2$. Therefore, the fabrication process of a metal contact, which aims for minimal contact resistance should force the semiconductor band gap to narrow by inserting metal induced states not far below the conduction band or not far above the valence band.

This work was supported by the EPSRC grants EP/I010084/1, EP/I009973/1, and HECToR facility computer resource EPSRC grant EP/F067496. PVS was supported by the Royal Society.

References

- [1] Truman J K and Holloway P H 1985 *J. Vac. Sci. Technol. A* **3** 992
- [2] Singiseti U, Wistey M A, Zimmerman J D, Thibeault B J, Rodwell M J, Gossard A C, and Bank S R 2008 *Appl. Phys. Lett.* **93** 183502
- [3] Jacoboni C and Lugli P 1989 *The Monte Carlo Method for Semiconductor Device Simulation* Wien-New York: Springer-Verlag
- [4] Aldegunde M, Seoane N, García-Loureiro A J and Kalna K 2010 *Comput. Phys. Commun.* **181** 24
- [5] Perdew J P, Burke K, and Ernzerhof M 1996 *Phys. Rev. Lett.* **77** 3865
- [6] Blöchl P E 1994 *Phys. Rev. B* **50** 17953
- [7] Kresse G and Furthmüller 1996 *Phys. Rev. B* **54** 11169
- [8] Dovesi R, Saunders V R, Roetti C, Orlando R, Zicovich-Wilson C M, Pascale F, Civalleri B, Doll K, Harrison N M, Bush I J, D'Arco P and Llunell M 2009 *CRYSTAL09 User's Manual* University of Torino, Torino
- [9] Weigend F and Ahlrichs R 2005 *Phys. Chem. Chem. Phys.* **7** 3927
- [10] Aldegunde M, Hepplestone S, Sushko P, and Kalna K 2014 *Semicond. Sci. Technol.* **29** 054003 (7pp).
- [11] Sun L, Liu X Y, Liu M, Du G and Han R Q 2003 *Semicond. Sci. Technol.* **18** 576
- [12] Razavy M 2003 *Quantum Theory of Tunneling* World Scientific
- [13] Rhoderick E H and Williams R H 1988 *Metal-Semiconductor Contacts* Oxford University Press
- [14] Sze S M and Ng K K 2006 *Physics of Semiconductor Devices* Wiley-Interscience
- [15] Kim S et al. 2013 *IEEE Trans. Nanotechnol.* **60** 2512
- [16] Zhou X, Li Q, Tang C W, and Lau K M 2012 *IEDM Tech. Dig.* 773